High Index Contrast Waveguides in Chalcogenide Glass and Polymer

Ray G. DeCorby, *Member, IEEE*, Nakeeran Ponnampalam, Mahesh M. Pai, Hue T. Nguyen, Prabhat K. Dwivedi, Thomas J. Clement, Chris J. Haugen, *Member, IEEE*, Jim N. McMullin, and Safa O. Kasap

***Abstract*—We review various properties of chalcogenide glasses that make them promising materials for passive and active microphotonics. We then describe two processes for channel waveguide fabrication, using the chalcogenide glass As_2Se_3 as a core material and compatible polymers as claddings. In the first approach, waveguides are patterned directly in the chalcogenide film by photoexposure through a mask followed by selective wet etching. This technique has produced shallow rib waveguides with losses as low as 0.26 dB/cm and small modal area photonic wire waveguides with losses on the order of 10 dB/cm. In the second approach, waveguide patterning is achieved by using an organic photoresist as a mask for selective photodoping of silver into the chalcogenide glass. Selective wet etching produced strip waveguides with smooth and highly vertical sidewalls. We report preliminary light guiding results for these latter structures.**

***Index Terms*—Amorphous semiconductors, integrated optics, optical planar waveguide components, optical strip waveguides, thin-film devices.**

I. Introduction

A MAJOR THEME within the field of integrated optics is realization of high index contrast waveguides and devices [1]. This research is sometimes termed microphotonics [2]. Its aims are the realization of chip-scale photonic devices and ultimately the integration of photonic and optoelectronic devices on microelectronic chips. Most of the work in microphotonics is targeted toward integration on silicon and especially monolithic integration of photonic elements with CMOS electronics. This strategy is motivated by trends in both the optical networking and computing industries, which point to a continued convergence of silicon and photonics.

1) Many of the control and signal processing functions in optical networks are performed by CMOS electronics circuitry. Much effort has been devoted to the development of all-optical devices and networks, but recently there has been a counterprevailing trend toward increased use of electronic signal processing (for regeneration, advanced coding techniques for error correction, etc.) in optical networks [3]. Integration of passive and active photonic functions with silicon electronics would enable increased penetration of optical transport into metro and access networks.
2) On-chip electrical interconnects are beginning to pose serious challenges to the continuation of Moore's Law growth of computing power [2]. As clock frequencies approach 10 GHz and on-chip wire dimensions shrink, it becomes increasingly difficult to provide synchronous clock to all sectors of a microprocessor chip. Further, heat generated in electrical interconnects is a significant practical challenge. While a range of approaches is under study to mitigate these issues, on-chip optical global interconnects might be necessary and feasible within the next decade or two [4]. Recent photonics research within the computing industry [5], [6] would seem to support this point of view.

Two approaches toward silicon microphotonics are possible. In the dominant approach to date, researchers have demonstrated active and passive photonic functions within the crystalline silicon layer of silicon-on-insulator (SOI) wafers [6]. A second, less-studied approach to microphotonics is to build passive and active photonic functions within the interconnect layers of electronic chips [7]–[9]. Fabrication steps of this nature are called back-end processes, and the processing temperatures must be restricted (to approximately 400 °C or less [10]) to avoid damaging underlying layers. Further, any materials or chemicals employed would need to be compatible with the overall process. While this poses significant practical challenges, building microphotonics in the interconnect layers offers the advantage of greater flexibility (customized materials; the possibility for three-dimensional photonic circuitry) and does not rob wafer real estate from the electronics.

For a glass-based microphotonics, the key requirement is a set of materials with high index contrast ($\Delta n > 1$ is required for bending radius less than 10 μm [2]). For a back-end process, materials that can be processed at relatively low temperatures are advantageous. High index contrast waveguide structures have been demonstrated in various amorphous or polycrystalline material systems, including Si [9], low-temperature deposited silicon oxy-nitride [7], silicon-rich silicon nitride [11], and tantalum oxide [12]. These materials have refractive indices ranging from approximately 2 to 3.5.

The chalcogenide glasses have refractive indices in the 2–3 range and are typically compatible with low-temperature processing. Further, they have promising characteristics for realization of active optical functions (switching, amplification, modulation, etc.). For these reasons, we have been investigating

Manuscript received July 16, 2004, revised February 1, 2005. This work was supported in part by the Natural Science and Engineering Research Council of Canada, in part by the Canadian Institute for Photonic Innovation, and in part by TRLabs.

R. G. DeCorby, N. Ponnampalam, M. M. Pai, H. T. Nguyen, P. K. Dwivedi, T. J. Clement, C. J. Haugen, and J. N. McMullin are with the Department of Electrical and Computer Engineering, University of Alberta, Edmonton, AB T6G 2V4, Canada, and also with TRLabs, Edmonton, AB T6G 2V4, Canada (e-mail: pnakeera@trlabs.ca).

S. O. Kasap is with the Electrical Engineering Department, University of Saskatchewan, Saskatoon, SK S7N 5A9, Canada.

Digital Object Identifier 10.1109/JSTQE.2005.845610

their potential as enablers of silicon-based microphotonics. In Section II, we provide a brief overview of chalcogenide glasses and their interesting properties for microphotonics, as well as a brief review of chalcogenide-glass-based integrated optics work reported in the literature. In Section III, we describe results obtained for high index contrast waveguide structures we have fabricated using a chalcogenide glass (As_2Se_3) and some commercially available polymers. Finally, in Section IV, we discuss some of the challenges associated with the present approach and some topics for future research.

II. Chalcogenide Glasses and Their Application in Integrated Optics—Background

A. Properties of Chalcogenide Glasses

Chalcogenide glasses have been the subject of much research and technological development over the past several decades [13], [14]. By the usual definition, they are alloys containing one or more of the elements S, Se, and Te. Ignoring the Te-based glasses (which are fairly opaque in the visible and near IR wavelength regions), typical binary glasses are As–S, As–Se, Ge–S, and Ge–Se. Ternary and quaternary glasses are often realized by combining these binary compositions or by addition of other elements such as Ga or Sb. Comparing the sulfide and selenide glasses, the sulfide glasses are typically characterized by a wider bandgap, higher glass transition temperature, lower density, greater hardness, and higher thermal conductivity [15]. Some of the interesting technological properties of chalcogenide glasses for integrated optics, many of them interrelated, are briefly summarized as follows.

1) As mentioned, the chalcogenide glasses have high refractive indices. This fact combined with their processing options has made them of interest for photonic crystal research. Photonic bandgap structures have been demonstrated in both planar [16] and fiber [17], [18] form.
2) Their relatively high atomic masses and weak bond strengths result in chalcogenide glasses having low characteristic phonon energies ($\sim$350–450 cm^{-1}), even relative to fluoride glasses ($\sim$ 550 cm^{-1}). Thus, chalcogenide glasses are highly transparent in the mid- to far IR, and they originally attracted technological and commercial interest for use in IR windows and optics [19]. On the other hand, chalcogenide glasses have narrow bandgaps ($\sim$ 2 eV) and relatively poor transparency (compared to oxide glasses) in the visible and UV wavelength regions. The transparency window of selenide glasses is approximately in the 0.8–15 μm wavelength range, while that of sulfide glasses is approximately in the 0.5–10-μm wavelength range.
3) Related to their "weak" bonding arrangements, chalcogenide glasses exhibit an array of photoinduced structural changes [13]. In some cases, these photoinduced effects are apparently unique to the chalcogenide glasses, while in other cases it is the magnitude of the effects (relative to similar effects in other glass systems) that is notable. Near bandgap light can be used to induce relatively large changes in glass absorption (photodarkening or photobleaching) and refractive index, useful in the patterning of gratings and waveguides. Further, such exposure typically modifies the physical structure of the glass and alters its etch characteristics, making chalcogenide glasses interesting as inorganic photoresists [16].
4) In the particularly unique photodoping, a metal film (typically silver) is deposited on a chalcogenide glass and light near the bandgap wavelength of the chalcogenide glass causes dissolution of the metal by the chalcogenide glass [14].
5) Another unique physical characteristic is the reversible amorphous to crystalline phase change that can be induced by controlled thermal cycling (through laser absorption or current flow) of certain chalcogenide alloys. The commercially successful rewritable CD/DVD is based on this property [20], as are the ovonic embedded memory elements under development by Intel and others. Indeed, chalcogenide films (Ge–Sb–Te) have already been monolithically integrated in a radiation hardened CMOS process [21].
6) Their mid-IR transparency, high refractive index, and low phonon energies make chalcogenide glasses of interest as hosts for rare-earth based amplifiers and lasers. Because of the low phonon energy, transitions that are quenched in most other glasses can exhibit high radiative efficiency in chalcogenide glasses. In particular, IR sources based on rare-earth doped chalcogenide glass [22] have attracted interest.
7) Related to their narrow bandgaps and high linear refractive index, chalcogenide glasses exhibit high nonlinearities in the near IR wavelength region [23]. With Kerr nonlinear coefficients two to three orders of magnitude higher than those of silicate glasses, chalcogenide glasses hold promise for realization of all-optical devices in fiber networks [24].
8) Certain chalcogenide alloys have high acoustooptic figures of merit and low acoustic loss. The earliest work on chalcogenide glass integrated optics was for acoustooptic applications [25]. Further, the chalcogenide glass $Ge_{33}As_{12}Se_{55}$ (AMTIR-1) is a standard material used for bulk acoustooptic cells operating in the near IR.

In summary, chalcogenide glasses have high refractive indices, are potentially compatible with back-end CMOS processing, provide numerous options for direct patterning of microstructures, and can potentially enable diverse active functionality. Key challenges to their use (at least for certain chalcogenide alloys) include toxicity, lack of chemical and mechanical durability [26], thermal expansion incompatibilities with certain substrates [27], and stability issues during processing [22] and under certain operational conditions [28].

B. Chalcogenide Glasses in Integrated Optics Research

The initial research on chalcogenide glasses for integrated optics was conducted in the 1970s. Ohmachi fabricated As_2S_3 thin films on a piezo-electric substrate (lithium niobate) and demonstrated an acoustooptic beam deflector [25]. In 1974, researchers at Texas Instruments reported slab and channel waveguide results for a few chalcogenide glass alloys (As_2S_3, $Ge_{28}Sb_{12}Se_{60}$, and $Ge_{33}As_{12}Se_{55}$), achieving propagation loss as low as 2 dB/cm

at 1064 nm wavelength [29]. In the late 1970s, Zembutsu *et al.* studied integrated optics devices using Ge–As–S–Se glass [30]. They reported propagation losses as low as 0.4 dB/cm at 1060-nm wavelength. At about the same time, Suhara *et al.* [31] studied passive grating elements, acoustooptic, and electrooptic devices employing As_2S_3 thin-film waveguides.

Rapid growth of fiber networks in the 1990s spurred renewed interest in materials for integrated optics. Starting in the late 1990s, researchers at Laval University, Quebec, QC, Canada, have been studying passive [26], [32] and nonlinear [28] integrated devices in chalcogenide glass, using mainly As_2S_3 and As–S–Se alloys. In 1997, Ramachandran *et al.* reported [27] the use of rapid thermal annealing as a means to achieve low loss channel waveguides in $Ge_{10}As_{40}S_{25}Se_{25}$ thin films. Recently, Zakery *et al.* [33] reported channel waveguide losses $< 0.2\,\mathrm{dB/cm}$ in As_2S_3 films fabricated by pulsed laser deposition. A research program at Lucent studied the use of chalcogenide glasses for nonlinear integrated optics [24], and interesting results were reported for $Ge_{25}Se_{75}$-based channel waveguides. In other work at Lucent, $Ge_{25}Se_{75}$ glass was used as a cladding material for quantum cascade lasers [34]. Balan *et al.* have studied the use of chalcogenide glass integrated waveguides for IR sensing applications [35].

Not least, we also mention work that has been conducted by researchers at the University of Southampton, Southampton, U.K., using Ga–La–S [36], [37] and Ge–S [38] glasses. These glasses have significant advantages relative to the arsenic-based glasses, including lower toxicity, greatly improved thermal and mechanical properties, and increased solubility for rare-earth dopants. One drawback is that there are fewer options for thin-film deposition of these alloys, although promising results were obtained by pulsed laser deposition [36] and chemical vapor deposition [38]. Recently, Mairaj *et al.* reported waveguide lasers formed by laser patterning of a bulk sample of Nd-doped Ga–La–S [37].

III. Results

While the majority of the previous research described in Section II was based on As_2S_3 glass, we have chosen As_2Se_3 glass for our initial work. As_2Se_3 is commercially available in bulk form and forms high-quality stoichiometric thin films by thermal evaporation. Further, it has a nearly optimal (amongst the chalcogenide glasses) nonlinear figure of merit and high nonlinear Kerr coefficient (nearly three orders of magnitude higher than silica glass) at 1550-nm wavelength [23]. We have used this glass to fabricate high index contrast waveguide structures, which is another distinguishing feature of this work relative to previously reported chalcogenide waveguides.

As_2Se_3 glass exhibits excellent thermomechanical compatibility with some polymers, which has enabled the realization of photonic bandgap fibers [17], [18]. Polysulfone [17], polyether sulfone and polyether imide [18] polymers have been combined with As_2Se_3 in that application. We have chosen a similar approach in our planar waveguide research. Two commercial polymers, a polyamide-imide or PAI (Torlon, Solvay Advanced Polymers) [39] and benzocyclobutene (BCB) (Cyclotene, Dow Polymers), were selected from a study of several commercial polymers. They were chosen based on their chemical, thermal, and mechanical compatibility with As_2Se_3. Mutual adhesion between thin films, especially on cleaving, was considered of prime importance. Also, the polymers were required to have good resistance to the wet chemicals used to etch the As_2Se_3 glass. Finally, a good coefficient of thermal expansion (CTE) match between materials is necessary to avoid film cracking and delamination [18]. The CTE is approximately $21\times10^{-6}\ \mathrm{C}^{-1}$, $30\times10^{-6}\ \mathrm{C}^{-1}$, and $52\times10^{-6}\ \mathrm{C}^{-1}$ for As_2Se_3, PAI, and BCB respectively. Further, the refractive indices are approximately 2.8, 1.6, and 1.5 for As_2Se_3, PAI, and BCB respectively. In the following subsections, results for three different types of waveguide structures are described.

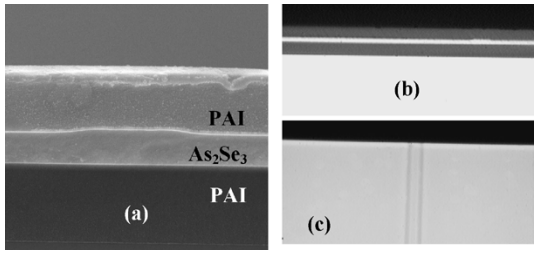

Fig. 1. (a) SEM image of the cleaved facet of a rib waveguide, with a rib width of approximately 3.8 μm. The color difference between the upper and lower PAI claddings is an artifact of SEM imaging. This difference is not visible in microscope images. (b) Microscope image showing the end view of a cleaved facet. A shallow rib is visible near the right-hand side of the image. (c) Microscope image showing the top view of a cleaved facet.

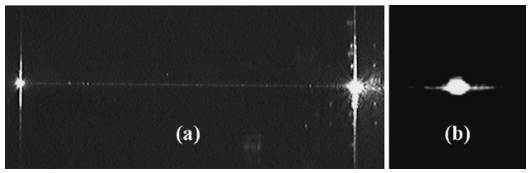

Fig. 2. (a) Scattered light streak from a 3.8-μm-wide rib waveguide; 980-nm-wavelength light was coupled in at the left side of the image. The guide shown is approximately 3 mm in length. (b) Light emanating from the end facet of the guide, imaged by a charge-coupled device (CCD) camera via an objective lens.

A. Shallow Rib Waveguides

Shallow rib waveguides do not provide strong lateral confinement, and are therefore not compatible with micrometer-scale bends. Compared to strip waveguides, however, rib waveguides are less sensitive to the roughness of etched sidewalls and typically exhibit lower scattering losses [40]. Further, it is possible to realize compact 90 degree bends in rib waveguides by use of etched corner reflectors [40].

A brief description of the fabrication process follows; further details can be found elsewhere [41]–[43]. First, a PAI undercladding ($\sim$ 2 μm thick) was deposited by spin casting on a silicon wafer, following the process described in [39]. Approximately 1 μm of As_2Se_3 glass was thermally evaporated onto the PAI undercladding. Waveguides were patterned directly in the as-deposited As_2Se_3 film, by exposure through a photomask in a standard UV mask aligner. The UV exposure photodarkens the As_2Se_3 and increases its resistance to certain etchants. A monoethanolamine (MEA)–based etchant was used to form shallow rib waveguides, by etching the unexposed glass to a depth of approximately 150 nm. Finally, an upper cladding of PAI was deposited by spin casting. An important

TABLE I
COMPARISON OF VARIOUS LOW-LOSS CHALCOGENIDE GLASS WAVEGUIDES REPORTED IN THE LITERATURE

Chalcogenide Alloy	Type of Waveguide	Transverse Core Dimensions [μm]	Wavelength [nm]	Reported Loss [dB/cm]	Reference
As_2S_3	Slab	0.7	1064	2	[29]
$Ge_{10}As_{40}Se_{10}S_{40}$	Slab	1	1060	0.4	[30]
As_2S_3/ $As_{24}Se_{38}S_{38}$	Etched shallow rib	1.25 x 5	1300	1	[26]
$Ge_{10}As_{40}Se_{25}S_{25}$	Laser written	1 x 5	1566	0.3	[27]
$Ge_{25}Se_{75}$	Laser written	1.7 x 3	1550	1.6	[24]
As_2S_3	Laser written	2.5 x 3.5	1550	0.2	[33]
As_2Se_3	Etched shallow rib	1 x 4	1530	0.26	[41]

factor in the selection of this polymer is that it can be cured at temperatures below the glass transition temperature of As_2Se_3 ($\sim 180^{\circ}C$). Fig. 1 shows scanning electron microscopy (SEM) and microscope images of a typical rib waveguide. One desirable aspect of our process is that the chalcogenide film is effectively annealed [27], without any evidence of cracking or delamination [33].

Waveguides with rib widths varying from 3.8 to 4.2 μm were fabricated. Simulations predicted that the 3.8-μm waveguides should be single moded at 1550 nm, while the wider guides tended to support two modes for each polarization. Light propagation was studied at 980-, 1480-, and 1530-nm wavelengths using various fiber pigtailed laser sources. Fig. 2 shows light propagation in a typical 3.8 μm wide guide at 980 nm. Fabry–Pérot loss measurements at 1530 nm on waveguides of various lengths revealed propagation losses as low as 0.26 dB/cm. Typical insertion loss, using a high numerical aperture (NA) fiber for input coupling, was $\sim$ 5.5 dB. Of this total modal mismatch coupling loss was estimated to contribute 4.7 dB. We were able to write first-order Bragg gratings in these guides, by holographic exposure (through the upper PAI cladding) with a HeNe laser. Stop bands with reflection greater than 20 dB were demonstrated, and we were able to accurately determine the modal characteristics of the guides from the wavelength positions of various stop bands. Details on all of these experiments have been reported elsewhere [41], [43]. Table I provides a summary of results for most of the thin-film chalcogenide glass waveguides reported in the literature.

B. Photonic Wire Waveguides

Embedded strip waveguides with very high index contrast between core and cladding are perhaps the key enablers for microphotonics [6]. These guides have been called photonic or optical wires. They are typically characterized by core-cladding index contrast $\Delta n > 1$ and submicrometer cross-sectional dimensions. Almost all of the work to date has been in the SOI material system. Using a similar fabrication approach to that described in the previous subsection, we have fabricated photonic wire strip waveguides comprising an As_2Se_3 core and polymer claddings. In this case, a BCB undercladding was chosen for its excellent resistance to the MEA-based etchant used to pattern the chalcogenide glass. Fig. 3 shows microscope and SEM images of a typical wire. Note that these guides have a shape reminiscent of a cylindrical lens. In fact, a similar fabrication process has been reported previously [16] for the manufacture of cylindrical lenses in As–Se glasses. As discussed in [16], the shape of the strip waveguides is a result of the interplay between exposure dose and etch rate. Also note from Fig. 3(a) that the guides contained visual defects, which we attribute to undercutting by the MEA etchant. We have tested and simulated the guides at 980-, 1480-, and 1530-nm wavelengths. The TE_0 mode is predicted to be highly confined to the core and suffered very high propagation loss due to scattering at defects. The TM_0 mode is somewhat less confined and exhibited lower loss. Fig. 4(a) shows the horizontal modal profiles of TE_0 and TM_0 modes at 1480 nm obtained by translating a detector, apertured by a 5-μm pinhole. The horizontal $1/e$ intensity width was measured as 2.7 and 4.5 μm for TE and TM modes, respectively. At 980 nm, modal area less than 1 μm^2 was predicted from simulations and partially verified by experiments [see Fig. 4(b)]. The resolving power of the optics used is on the order of 1 μm. The propagation loss was estimated by Fabry–Pérot measurements, scattered light measurements [Fig. 4(c) and (d)], and from an analysis

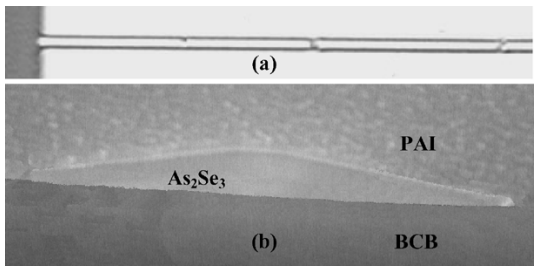

Fig. 3. (a) Microscope top image of an As_2Se_3 photonic wire waveguide embedded in polymer claddings, near a cleaved facet. (b) SEM image showing the end view of a chalcogenide glass strip embedded in polymer. The strip has a circle-segment cross section, with width approximately 800 nm and maximum thickness approximately 180 nm.

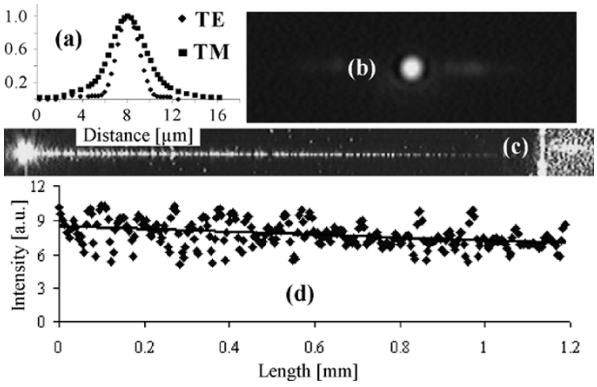

Fig. 4. (a) Horizontal mode profile of TE_0 and TM_0 modes at 1480 nm, obtained by scanning an apertured photodetector through the magnified near-field image. (b) 980-nm light emanating from the facet of a photonic wire waveguide, imaged by a CCD camera via an objective lens. (c) 980-nm scattered light streak for the same waveguide. The total length of the guide shown is approximately 2.4 mm. The bright area near the right side of the image is partially due to reflections from the objective lens used to collect light at the output facet. (d) Intensity distribution at 980 nm along the length of the waveguide.

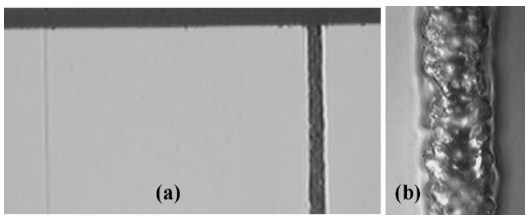

Fig. 5. (a) Microscopic image showing a damaged photonic wire waveguide (right side) adjacent to an intact waveguide (left side). The output facet of the waveguides is shown. (b) Higher magnification image of the damaged waveguide.

of the contributions to total insertion loss. All of these techniques produced estimates for propagation loss of 10–15 dB/cm, which compares well with results reported for SOI photonic wire waveguides [6]. Further, we believe that significant optimization is possible. Improved control of the glass exposure and etching process should reduce the number of scattering defects. Also, the waveguide geometry can be optimized to provide a desired level of modal confinement. Given that organic photoresist processing is a significant contributor to line edge roughness and resultant scattering loss in small waveguides [44], it is potentially advantageous that the process described here does not involve organic resists.

As an initial assessment of stability, we tested both the rib and wire waveguides under moderately high continuous wave power. Approximately 35 mW at 1480 nm was coupled into the guides, and the output power was monitored over extended periods (up to several days). In most cases, the waveguides did not exhibit any apparent degradation, as evidenced by monitoring the output power. In one interesting case only, these launch conditions destroyed a photonic wire waveguide as shown in Fig. 5. We speculate that this was due to a waveguide "fuse" process, such as has been observed in silica and chalcogenide fibers previously [45]. It is possible that dust on the output facet caused enough local heating to initiate the fuse process.

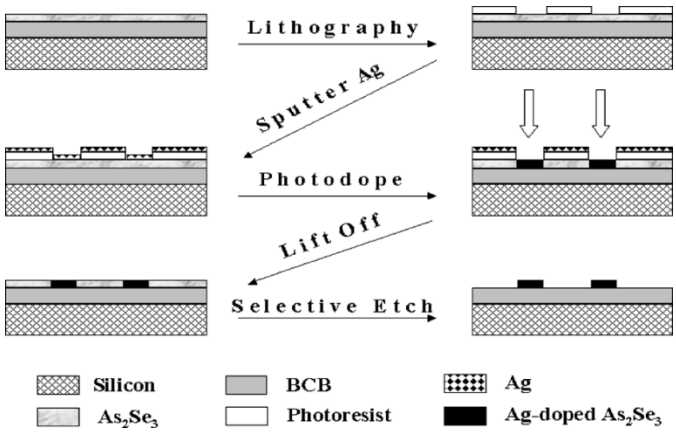

Fig. 6. Block diagram illustrating the processing steps used in the fabrication of Ag-doped strip waveguides.

C. Ag-Doped Strip Waveguides

As compared to photodarkening, metal doping of As_2Se_3 films not only gives a higher index change ($\Delta n > 0.3$ is possible [14]) but also results in higher wet-etch selectivity between doped and undoped regions. After a metal is patterned on a chalcogenide film, its dissolution can be induced thermally or optically [46]. Photodoping is potentially a unique enabler of microphotonics [14], but remains relatively unexplored for this purpose. It is possible to selectively photodope regions of a chalcogenide glass film by illumination through a mask. As compared to thermal doping, in photodoping the lateral diffusion of metal is minimal (under the right conditions), and thus high resolution can be achieved. A unique characteristic is that highly anisotropic and vertical etch features can be realized in a wet-etch process [47]. A second motivation for studying photodoped waveguides is that Ag-doped glasses have emerged as a promising medium for third-order nonlinear optics. Ultrafast Kerr nonlinearities three to four orders of magnitude higher than in silica glass have been reported for Ag–Ga–Ge–S [48] and Ag–As–Se [49] alloys.

We patterned multimoded strip waveguides by using a liftoff process, as illustrated in Fig. 6. It has been observed in our work [42] that the Ag-As_2Se_3 interaction proceeds both during and after deposition of the metal even at room temperature. The high rate of interaction between As_2Se_3 and Ag necessitates selective deposition of Ag on to the chalcogenide film, and hence a liftoff process was used. The fabrication process started with deposition of a BCB undercladding on a cleaned silicon wafer. Approximately 0.7 μm of As_2Se_3 was subsequently deposited by thermal evaporation, at room temperature. HPR504 photoresist was spuncast onto the as-deposited chalcogenide film, and waveguide patterns were defined in the photoresist using a standard process. A thin layer (30 nm) of Ag was sputtered onto the patterned wafer and then the sample was flood exposed for 15 min, using the UV source in a standard mask aligner. The photoresist was then lifted off, and any remaining silver was removed by a quick dip in a silver etchant and a rinse with deionized water. The undoped chalcogenide region was then completely etched away using an amine-based etchant, producing the Ag-doped chalcogenide strip waveguides shown in Fig. 7. No upper cladding was deposited on these waveguides. Note

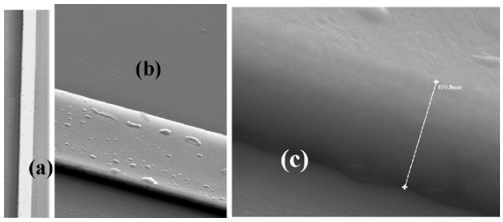

Fig. 7. (a) Microscope image of an Ag-doped strip waveguide, approximately 8 μm wide. (b) SEM image of an Ag-doped strip waveguide. The scale bar at upper right represents 1 μm. The features on the waveguide surface are possibly deposits of pure silver. (c) SEM image of the waveguide sidewall. The scale bar at upper right represents 100 nm.

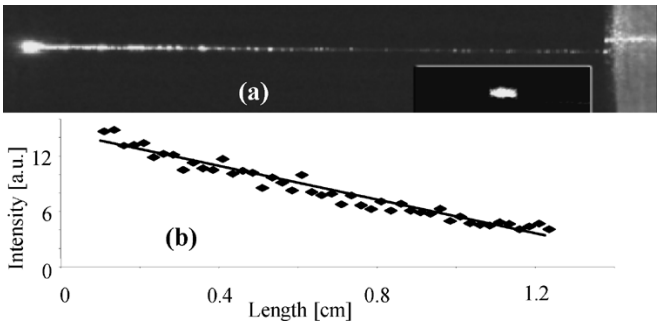

Fig. 8. (a) 980-nm scattered light from an Ag-doped strip waveguide, with total length approximately 5 mm. The objective lens used to gather light from the output facet can be seen at the right. Inset: 980-nm light emanating from the output facet, imaged by an objective lens and CCD camera. (b) Intensity distribution along the length of the waveguide at 1480 nm.

that the waveguide sidewalls are quite vertical and reasonably smooth.

In preliminary experiments, light guiding was studied in strip waveguides with widths greater than 8 μm. As shown in Fig. 8, the Ag-doped guides show strong guidance of 980-nm light. Analysis of scattered light images at 1480 nm, using a pickup fiber [Fig. 8(b)], produced an estimate for the propagation loss of ~ 9 dB/cm. Losses at 980 nm were much higher. As_2Se_3 exhibits bulk absorption in the 2–4 dB/cm range at 980 nm [42], and Ag-doping is known to decrease the bandgap of the glass. Thus, some portion of the measured propagation loss can be attributed to material absorption.

IV. Conclusion

We have demonstrated that low-loss, high index contrast waveguides can be realized using As_2Se_3 chalcogenide glass and commercial polymers. Waveguide patterning was achieved through photo-induced etch resistance of the chalcogenide glass film, in some cases without the use of organic photoresists. Since photoresist patterning and development is a major source of scattering loss in microphotonics, avoidance of these steps is a potential advantage. The materials we have employed offer a core-cladding index offset $\Delta n > 1$. With further optimization of waveguide geometry, this should enable single-mode waveguides with submicrometer modal area and bending radius in the micrometer regime.

Outstanding questions remain with respect to stability, particularly for the As_2Se_3 glass used in this work. The relatively low glass transition temperature of this glass ($T_g \sim 180$ °C) suggests that thermal stability could be a problem. Perhaps of greater concern is the stability under light exposure. While the photo-structural changes exhibited by chalcogenide glasses are useful in device fabrication, they might lead to stability concerns during device operation. Ho *et al.* [28] have demonstrated that As_2S_3 glass films can be photodarkened by intense subbandgap light at 1550-nm wavelength. Similar problems would potentially be encountered in the narrower bandgap As_2Se_3 glass. Several alternative chalcogenide alloys, such as Ga–Ge–S and Ga–La–S [37], offer superior thermomechanical properties compared to As_2Se_3 while maintaining most of the interesting properties that enabled the work described here.

Acknowledgment

The authors would like to thank G. Braybrook for capturing excellent SEM images. The devices were fabricated at the Nanofab, University of Alberta, Edmonton, AB, Canada.

References

[1] C. Manolatou, S. G. Johnson, S. Fan, P. R. Villeneuve, H. A. Haus, and J. D. Joannopoulos, "High-density integrated optics," *J. Lightw. Technol.*, vol. 17, no. 9, pp. 1682–1692, Sep. 1999.

[2] L. C. Kimerling, "Silicon microphotonics," *Appl. Surf. Sci.*, vol. 159–160, pp. 8–13, 2000.

[3] K. Azadet, E. F. Haratsch, H. Kim, F. Saibi, J. H. Saunders, M. Shaffer, L. Song, and M.-L. Yu, "Equalization and FEC techniques for optical transceivers," *IEEE J. Solid-State Circuits*, vol. 37, no. 3, pp. 317–327, Mar. 2002.

[4] A. V. Mule, E. N. Glytsis, T. K. Gaylord, and J. D. Meindl, "Electrical and optical clock distribution networks for gigascale microprocessors," *IEEE Trans. Very Large Scale (VLSI) Syst.*, vol. 10, no. 5, pp. 582–594, Oct. 2002.

[5] G. T. Reed, "The optical age of silicon," *Nature*, vol. 427, pp. 595–596, 2004.

[6] Y. A. Vlasov and S. J. McNab, "Losses in single-mode silicon-on-insulator strip waveguides and bends," *Opt. Express*, vol. 12, no. 8, pp. 1622–1631, 2004.

[7] U. Hilleringmann and K. Goser, "Optoelectronic system integration on silicon: Waveguides, photodetectors, and VLSI CMOS circuits on one chip," *IEEE Trans. Electron Devices*, vol. 42, no. 5, pp. 841–846, May 1995.

[8] V. Stenger and F. R. Beyette, "Design and analysis of an optical waveguide tap for silicon CMOS circuits," *J. Lightw. Technol.*, vol. 20, no. 2, pp. 277–284, Feb. 2002.

[9] A. M. Agarwal, L. Liao, J. S. Foresi, M. R. Black, X. Duan, and L. C. Kimerling, "Low-loss polycrystalline silicon waveguides for silicon photonics," *J. Appl. Phys.*, vol. 80, no. 11, pp. 6120–6123, 1996.

[10] S. Sedky, A. Witvrouw, H. Bender, and K. Baert, "Experimental determination of the maximum post-process annealing temperature for standard CMOS wafers," *IEEE Trans. Electron Devices*, vol. 48, pp. 377–385, 2001.

[11] H. T. Philipp, K. N. Anderson, W. Svendsen, and H. Ou, "Amorphous silicon rich silicon nitride optical waveguides for high density integrated optics," *Electron. Lett.*, vol. 40, no. 7, pp. 419–421, Apr. 2004.

[12] C.-Y. Tai, C. Grivas, and J. S. Wilkinson, "UV photosensitivity in a Ta_2O_5 rib waveguide Mach–Zehnder interferometer," *IEEE Photon. Technol. Lett.*, vol. 16, no. 6, pp. 1522–1524, Jun. 2004.

[13] A. Zakery and S. R. Elliot, "Optical properties and applications of chalcogenide glasses: A review," *J. Non-Cryst. Solids*, vol. 330, pp. 1–12, 2003.

[14] M. Frumar and T. Wagner, "Ag doped chalcogenide glasses and their applications," *Curr. Opin. Solid State Mater. Sci.*, vol. 7, pp. 117–126, 2003.

[15] A. R. Hilton and D. J. Hayes, "The interdependence of physical parameters for infrared transmitting glasses," *J. Non-Cryst. Solids*, vol. 17, pp. 339–348, 1975.

[16] V. Lyubin, M. Klebanov, A. Feigel, and B. Sfez, "Films of chalcogenide glassy semiconductors: New phenomena and new applications," *Thin Solid Films*, vol. 459, pp. 183–186, 2004.

[17] D. J. Gibson and J. A. Harrington, "Extrusion of hollow waveguide performs with a one-dimensional photonic bandgap structure," *J. Appl. Phys.*, vol. 95, no. 8, pp. 3895–3900, 2004.
[18] K. Kuriki, O. Shapira, S. D. Hart, G. Benoit, Y. Kuriki, J. F. Viens, M. Bayindir, J. D. Joannopoulos, and Y. Fink, "Hollow multilayer photonic bandap fibers for NIR applications," *Opt. Express*, vol. 12, no. 8, pp. 1510–1517, 2004.
[19] X. H. Zhang, Y. Guimond, and Y. Bellec, "Production of complex chalcogenide glass optics by molding for thermal imaging," *J. Non-Cryst. Solids*, vol. 326–327, pp. 519–523, 2003.
[20] M. Naito, M. Ishimaru, and Y. Hirotsu, "Local structure analysis of Ge–Sb–Te phase change materials using high-resolution electron microscopy and nanobeam diffraction," *J. Appl. Phys.*, vol. 95, no. 12, pp. 8130–8135, 2004.
[21] J. D. Maimon, K. K. Hunt, L. Burcin, and J. Rodgers, "Chalcogenide memory arrays: Characterization and radiation effects," *IEEE Trans. Nucl. Sci.*, vol. 50, no. 6, pp. 1878–1884, Dec. 2003.
[22] L. B. Shaw, B. Cole, P. A. Thielen, J. S. Sanghera, and I. D. Aggarwal, "Mid-wave IR and long-wave IR laser potential of rare-earth doped chalcogenide glass fiber," *IEEE J. Quantum Electron.*, vol. 48, no. 9, pp. 1127–1137, Sep. 2001.
[23] R. E. Slusher, G. Lenz, J. Hodelin, J. Sanghera, L. B. Shaw, and I. D. Aggarwal, "Large Raman gain and nonlinear phase shifts in high-purity As_2Se_3 chalcogenide fibers," *J. Opt. Soc. Amer. B*, vol. 21, no. 6, pp. 1146–1155, 2004.
[24] S. Spalter, H. Y. Hwang, J. Zimmerman, G. Lenz, T. Katsufuji, S.-W. Cheong, and R. E. Slusher, "Strong self-phase modulation in planar chalcogenide glass waveguides," *Opt. Lett.*, vol. 27, no. 5, pp. 363–365, 2002.
[25] Y. Ohmachi, "Acousto-optical light diffraction in thin films," *J. Appl. Phys.*, vol. 44, no. 9, pp. 3928–3933, 1973.
[26] J.-F. Viens, C. Meneghini, A. Villeneuve, T. V. Galstian, E. J. Knystautas, M. A. Duguay, K. A. Richardson, and T. Cardinal, "Fabrication and characterization of integrated optical waveguides in sulfide chalcogenide glasses," *J. Lightw. Technol.*, vol. 17, no. 7, pp. 1184–1191, Jul. 1999.
[27] S. Ramachandran and S. G. Bishop, "Low loss photoinduced waveguides in rapid thermally annealed films of chalcogenide glasses," *Appl. Phys. Lett.*, vol. 74, no. 1, pp. 13–15, 1999.
[28] N. Ho, J. M. Laniel, R. Vallee, and A. Villeneuve, "Photosensitivity of As_2S_3 chalcogenide thin films at 1.5 μm," *Opt. Lett.*, vol. 28, no. 12, pp. 965–967, 2003.
[29] R. K. Watts, M. de Wit, and W. C. Holton, "Nonoxide chalcogenide glass films for integrated optics," *Appl. Opt.*, vol. 13, no. 10, pp. 2329–2332, 1974.
[30] S. Zembutsu and S. Fukunishi, "Waveguiding properties of (Se,S)- based chalcogenide glass films and some applications to optical waveguide devices," *Appl. Opt.*, vol. 18, no. 3, pp. 393–399, 1979.
[31] T. Suhara and H. Nishihara, "Integrated optics components and devices using periodic structures," *IEEE J. Quantum Electron.*, vol. QE-22, no. 6, pp. 845–867, Jun. 1986.
[32] R. Vallee, S. Frederick, K. Asatryan, M. Fischer, and T. Galstian, "Real-time observation of Bragg grating formation in As_2S_3 chalcogenide rib waveguides," *Opt. Commun.*, vol. 230, pp. 301–307, 2004.
[33] A. Zakery, Y. Ruan, A. V. Rode, M. Samoc, and B. Luther-Davies, "Low-loss waveguides in ultrafast laser-deposited As_2S_3 chalcogenide films," *J. Opt. Soc. Amer. B.*, vol. 20, no. 9, pp. 1844–1852, 2003.
[34] C. Gmachl, H. Y. Hwang, R. Paiella, D. L. Sivco, J. N. Baillargeon, F. Capasso, and A. Y. Cho, "Quantum cascade lasers with low-loss chalcogenide lateral waveguides," *IEEE Photon. Technol. Lett.*, vol. 13, no. 3, pp. 182–184, Mar. 2001.
[35] V. Balan, C. Vigreux, A. Pradel, A. Llobera, C. Dominguez, M. I. Alonso, and M. Garriga, "Chalcogenide glass-based rib ARROW waveguide," *J. Non-Cryst. Solids*, vol. 326–327, pp. 455–459, 2003.
[36] D. S. Gill, R. W. Eason, C. Zaldo, H. N. Rutt, and N. A. Vainos, "Characterization of Ga–La–S chalcogenide glass thin-film optical waveguides, fabricated by pulsed laser deposition," *J. Non-Cryst. Solids*, vol. 191, pp. 321–326, 1995.
[37] A. K. Mairaj, A. M. Chardon, D. P. Shepherd, and D. W. Hewak, "Laser performance and spectroscopic analysis of optically written channel waveguides in neodymium-doped gallium lanthanum sulphide glass," *IEEE J. Sel. Topics Quantum Electron.*, vol. 8, no. 6, pp. 1381–1388, Nov./Dec. 2002.
[38] C. C. Huang, D. W. Hewak, and J. V. Badding, "Deposition and characterization of germanium sulphide glass planar waveguides," *Opt. Express*, vol. 12, no. 11, pp. 2501–2506, 2004.
[39] R. M. Bryce, H. T. Nguyen, P. Nakeeran, T. Clement, C. J. Haugen, R. R. Tykwinski, R. G. DeCorby, and J. N. McMullin, "Polyamide-imide polymer thin films for integrated optics," *Thin Solid Films*, vol. 458, pp. 233–236, 2004.
[40] S. Lardenois, D. Pascal, L. Vivien, E. Cassan, S. Laval, R. Orobtchouk, M. Heitzmann, N. Bouzaida, and L. Mollard, "Low-loss submicrometer silicon-on-insulator rib waveguides and corner mirrors," *Opt. Lett.*, vol. 28, no. 13, pp. 1150–1152, 2003.
[41] N. Ponnampalam, R. G. DeCorby, H. T. Nguyen, P. K. Dwivedi, C. J. Haugen, J. N. McMullin, and S. O. Kasap, "Small core rib waveguides with embedded gratings in As_2Se_3 glass," *Opt. Express*, vol. 12, no. 25, pp. 6270–6277, Dec. 2004.
[42] R. M. Bryce, H. T. Nguyen, P. Nakeeran, R. G. DeCorby, P. K. Dwivedi, C. J. Haugen, J. N. McMullin, and S. O. Kasap, "Direct UV patterning of waveguide devices in As_2Se_3 thin films," *J. Vac. Sci. Technol. A*, vol. 22, no. 3, pp. 1044–1047, 2004.
[43] N. Ponnampalam, R. G. DeCorby, H. T. Nguyen, P. K. Dwivedi, C. J. Haugen, J. N. McMullin, R. M. Bryce, and S. O. Kasap, "Low loss waveguides and embedded Bragg gratings in As_2Se_3 chalcogenide glass," presented at the Optical Soc. Amer. Integrated Photonics Research Topical Meeting, San Francisco, CA, 2004.
[44] T. Barwicz and H. I. Smith, "Evolution of line-edge roughness during fabrication of high-index-contrast microphotonic devices," *J. Vac. Sci. Technol. B*, vol. 21, no. 6, pp. 2892–2896, 2003.
[45] E. M. Dianov, I. A. Bufetov, A. A. Frolov, V. M. Mashinsky, V. G. Plotnichenko, M. F. Churbanov, and G. E. Snopatin, "Catastrophic destruction of fluoride and chalcogenide optical fibers," *Electron. Lett.*, vol. 38, no. 15, pp. 783–784, 2002.
[46] J. Fick, B. Nicolas, C. Rivero, K. Elshot, R. Irwin, K. A. Richardson, M. Fischer, and R. Vallee, "Thermally activated silver diffusion in chalcogenide thin films," *Thin Solid Films*, vol. 418, pp. 215–221, 2002.
[47] H.-Y. Lee and T. Yao, "Wet-etching selectivity of Ag-photodoped As-GeSeS thin films and the fabrication of a planar corrugated one-dimensional photonic crystal by a holographic method," *J. Vac. Sci. Technol. B.*, vol. 20, no. 5, pp. 2017–2023, 2002.
[48] D. Marchese, M. de Sario, A. Jha, A. K. Kar, and E. C. Smith, "Highly nonlinear GeS_2-based chalcohalide glass for all-optical twin-core-fiber switching," *J. Opt. Soc. Amer. B*, vol. 15, no. 9, pp. 2361–2370, 1998.
[49] K. Ogusu, J. Yamasaki, S. Maeda, M. Kitao, and M. Minakata, "Linear and nonlinear optical properties of Ag–As–Se chalcogenide glasses for all- optical switching," *Opt. Lett.*, vol. 29, no. 3, pp. 265–267, 2004.

Ray G. DeCorby (S'96–M'97) received the M.Sc. degree in electrical engineering from the University of Saskatchewan, Saskatoon, SK, Canada, in 1995 and the Ph.D. degree in electrical and computer engineering from the University of Alberta, Edmonton, AB, Canada, in 1998.

Currently, he is an Associate Professor of Electrical and Computer Engineering at the University of Alberta and a Scientist with TRLabs, Edmonton. His research interests include integrated optics on silicon platforms, photonic glasses and polymers, and integrated nonlinear optics.

Dr. DeCorby is a Member of the Optical Society of America.

Nakeeran Ponnampalam received the B.Sc. in electrical and electronic engineering from the University of Peradeniya, Sri Lanka, in 1999. He is currently working toward the Ph.D. degree in electrical and computer engineering at the University of Alberta, Edmonton, AB, Canada, and doing his research at TRLabs, Edmonton.

His research interests are photonic devices and integrated optics.

Mahesh M. Pai received the B.Tech degree in electrical engineering from the Indian Institute of Technology, Madras, in 2002. He is currently working toward the M.S. degree in electrical and computer engineering at the University of Alberta, Edmonton, AB, Canada, and TRLabs, Edmonton.

He is currently investigating high index contrast structures in chalcogenide glass. His research interests include ring-resonator-based multifunctional integrated optical circuits and integrated nonlinear optics.

Hue T. Nguyen received the B.Sc degree with specialization in Chemistry from the University of Alberta, Edmonton, AB, Canada, in 2000.

After receiving her B.Sc degree, she joined the Photonics Research Group of TRLabs, Edmonton. She is currently a Research Associate in the Photonics Group of TRLabs specializing in micro- and nanofabrication techniques.

Prabhat K. Dwivedi received the Ph.D. degree in physics from Harcourt Butler Technological Institute, Kanpur, India, in 1995, in the area of amorphous semiconductors.

He joined the Department of Physics, Indian Institute of Technology, Kanpur, as a Senior Project Scientist. His research there focused on thermal and photo irradiation induced changes in chalcogenides glasses. In addition, he published several papers based on his research. In 2001, he joined the Department of Electrical and Computer Engineering, University of Alberta, Edmonton, AB, Canada, as a Research Associate and TRLabs Visiting Scientist. His research interests include amorphous chalcogenide glasses (structure, properties, and possible applications) and its thin-film development by different methods for photonic applications.

Thomas J. Clement received the B.S. degree in electrical engineering from the University of Alberta, Edmonton, AB, Canada, in 2003. He is currently working toward the M.S. degree in electrical engineering at the University of Alberta in conjunction with TRLabs, Edmonton.

His research focuses on characterizing the optical properties of novel materials for application in telecommunication and electronics.

Chris J. Haugen (S'88–M'89) received the Ph.D. degree in electrical engineering from the University of Saskatchewan, Saskatoon, Canada, in 1998.

He was the Codes and Standards Engineer for the Electrical Regulatory Authority, Province of Saskatchewan, Canada. He joined TRLabs, Edmonton, AB, Canada, in 1999, where he is a Staff Researcher in the Photonics Research Group. In addition to carrying out his own research, his responsibilities at TRLabs include helping to define the overall photonics research program and supervising the various technicians, graduate, and undergraduate students conducting photonics research at TRLabs. He is also an Adjunct Professor in the Department of Electrical and Computer Engineering, University of Alberta, Edmonton. He has taught courses on introductory electronics, material science, microwave engineering, and fiber-optic communications. He has published several papers on the physical, electronic, and optical properties of materials and devices.

Dr. Haugen is a member of the Optical Society of America (OSA), and he is a registered professional engineer in the provinces of Alberta and Saskatchewan, Canada.

Jim N. McMullin received the Ph.D. degree in physics and astronomy from the University of Rochester, Rochester, NY, in 1975.

He is currently with the Department of Electrical and Computer Engineering, University of Alberta, Edmonton, AB, Canada, and also with TRLabs, Edmonton. He has over 100 published journal and conference papers in the areas of solar physics, plasma physics, semiconductor physics, fiber optics, and integrated optics and simulation techniques. From 1975 to 1983, he was involved in plasma fusion research. From 1983 to 1990, he studied light propagation in optical fibers and since then, the propagation of light in integrated and microoptics for telecommunications and microfluidic lab-on-a-chip applications.

Safa O. Kasap received the B.Sc. (in engineering), M.Sc., Ph.D., and D.Sc. (in engineering) degrees from Imperial College of Science, Technology and Medicine, University of London, U.K., in 1976, 1978, 1983, and 1996, respectively, specializing in amorphous semiconductors.

He is currently a Professor and Canada Research Chair in Electronic Materials and Devices in the Electrical Engineering Department, University of Saskatchewan, Saskatoon, SK, Canada. His textbooks *Principles of Electronic Materials and Devices, Second Edition* (Boston, MA: McGraw-Hill, 2002) and *Optoelectronics and Photonics: Principles and Practices* (Upper Saddle River, NJ: Prentice-Hall, 2001) are widely used at various universities and by many professionals worldwide. He is currently the Reviews Editor and the Deputy Editor for the *Journal of Materials Science: Materials in Electronics.* His research interests are in amorphous semiconductors, noise in electronic devices, photoconductors, photodetectors, X-ray image detectors, laser-induced transient photoconductivity, and related topics, with more than 100 refereed journal publications in these areas.

Dr. Kasap is a Fellow of the Institution of Electrical Engineers, the Institute of Physics, and the Institute of Materials.